

Dynamical deformation effects in subbarrier fusion of $^{64}\text{Ni} + ^{132}\text{Sn}$

A. S. Umar and V. E. Oberacker

Department of Physics and Astronomy, Vanderbilt University, Nashville, Tennessee 37235, USA

(Received 25 September 2006; published 22 December 2006)

We show that dynamical deformation effects play an important role in fusion reactions involving the ^{64}Ni nucleus, in particular the $^{64}\text{Ni} + ^{132}\text{Sn}$ system. We calculate fully microscopic interaction potentials and the corresponding subbarrier fusion cross-sections.

DOI: [10.1103/PhysRevC.74.061601](https://doi.org/10.1103/PhysRevC.74.061601)

PACS number(s): 25.70.Jj, 21.60.Jz, 24.10.-i, 25.70.Gh

Recently observed enhanced subbarrier fusion cross-sections for the neutron rich $^{64}\text{Ni} + ^{132}\text{Sn}$ system [1] has further invigorated the research in low-energy nuclear reactions involving exotic nuclei. For this system fusion cross-sections were measured in the energy range $142 \text{ MeV} \leq E_{\text{c.m.}} \leq 176 \text{ MeV}$. In particular, it was found that fission is negligible for $E_{\text{c.m.}} \leq 160 \text{ MeV}$ and therefore the evaporation residue cross-sections have been taken as fusion cross-sections. The enhancement of subbarrier fusion was deduced from comparison with a barrier penetration calculation, using a phenomenological Woods-Saxon interaction potential whose parameters were fitted to reproduce the evaporation residue cross-sections for the $^{64}\text{Ni} + ^{132}\text{Sn}$ system. Similarly, sophisticated coupled-channel calculations [2,3], which are known to enhance the fusion cross-sections by considering coupling to various excitation channels and neutron transfer, have significantly underestimated the subbarrier fusion cross-sections for the $^{64}\text{Ni} + ^{132}\text{Sn}$ system [1].

In general, the fusion cross-sections depend on the interaction potential and form factors in the vicinity of the Coulomb barrier. These are expected to be modified during the collision because of dynamical effects. In addition, experiments on subbarrier fusion have demonstrated a strong dependence of the total fusion cross-section on nuclear deformation [4]. The dependence on nuclear orientation has received particular attention for the formation of heavy and superheavy elements [5] and various entrance channel models have been developed to predict its role in enhancing or diminishing the probability for fusion [6,7].

Recently, we developed a new approach for calculating heavy-ion interaction potentials that incorporates all of the dynamical entrance channel effects included in the time-dependent Hartree-Fock (TDHF) description of the collision process [8]. These effects include the neck formation, particle exchange, internal excitations, and deformation effects to all orders, as well as the effect of nuclear alignment for deformed systems [7,8]. The method is based on the TDHF evolution of the nuclear system coupled with density-constrained Hartree-Fock (DCHF) calculations [9,10] to obtain the interaction potential. The density constrained TDHF method follows the unhindered dynamical TDHF trajectory in relation to the multidimensional static energy surface of the composite nuclear system to obtain the ion-ion potentials. In this regard the method is non-adiabatic in nature. The resulting potential is given by

$$V(R) = E_{\text{DC}}(R) - E_{A_1} - E_{A_2}. \quad (1)$$

The potential deduced from Eq. (1) contains *no parameters* and *no normalization*. Given an effective interaction, such as the Skyrme force, $V(R)$ can be constructed by performing a TDHF evolution and minimizing the energy at certain times to obtain $E_{\text{DC}}(R)$, while the nuclear binding energies E_{A_1} and E_{A_2} are the results of a static Hartree-Fock calculation with the same effective interaction [8]. Of course, in the absence of a true many-body tunneling approach to subbarrier fusion, our approach, as well as other macroscopic and microscopic methods, is based on various assumptions regarding the determination of the barrier and is somewhat speculative in nature.

We carried out a number of TDHF calculations with accompanying density constraint calculations to compute $V(R)$ given by Eq. (1). A detailed description of our new three-dimensional unrestricted TDHF code has recently been published in Ref [11]. For the effective interaction we used the Skyrme SLy5 force [12] including all of the time-odd terms. In our case the ^{64}Ni nucleus is essentially oblate with a small mix of triaxiality, having a quadrupole moment of -0.45 b . This is also confirmed by other calculations [13,14] and suggested by other experiments [15].

TDHF calculations were initialized at $E_{\text{c.m.}} = 158 \text{ MeV}$. In Ref. [8] we show that the calculation of the potential barrier is not sensitive to the choice of the TDHF initialization energy above the barrier, the only difference being a slightly lower potential well for lower energies. In Fig. 1 we show the results obtained for the interaction potential as well as the empirical potential barrier used in Ref. [1]. The angle β indicates the orientation of the symmetry axis. In the case of $\beta = 0^\circ$ the symmetry axis of the oblate ^{64}Ni is aligned with the collision axis and for $\beta = 90^\circ$ the symmetry axis is perpendicular to the collision axis. For the case of parallel orientation the calculated barrier is almost exactly the same as the one used in Ref. [1], having a barrier height of 155.8 MeV . The difference for smaller R values is due to the use of the point Coulomb interaction in the model calculation, which is unphysical when nuclei overlap. The same argument applies to small differences at large R values, because the Coulomb interaction is slightly different because of the deformed Ni nucleus. We would like to emphasize again that our calculations do not contain any parameters or normalization. On the other hand, the barrier corresponding to the perpendicular alignment is considerably lower, peaking at 150.1 MeV , and has a narrower width.

The physical picture that emerges from these calculations is that, for center-of-mass energies in the range

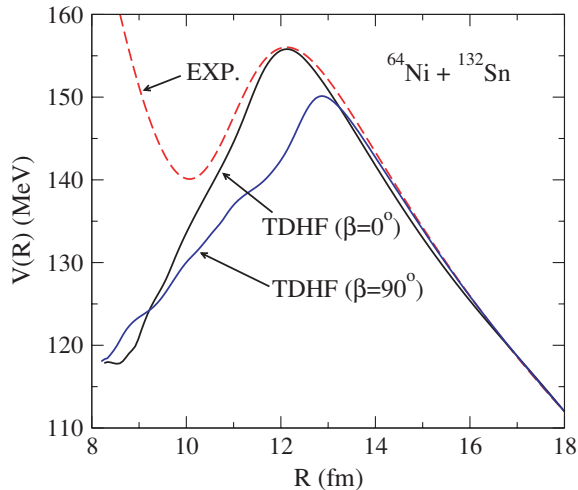


FIG. 1. (Color online) Internuclear potential obtained from Eq. (1) for the head-on collision of the $^{64}\text{Ni} + ^{132}\text{Sn}$ system at $E_{\text{c.m.}} = 158$ MeV. The dashed line shows the empirical Woods-Saxon potential used in Ref. [1].

150.1–155.8 MeV, the fusion cross-section would be dominated by the channel above the lower barrier because the contribution via tunneling through the higher barrier will be substantially smaller. Similarly, for energies below 150.1 MeV, transmission through the lower barrier will produce the dominant contribution. Of course, for energies above 155.8 MeV, both barriers will contribute. As a result, the only data point that is truly subbarrier is the lowest energy point.

In Fig. 2 we show the calculated fusion cross-sections as a function of the center-of-mass energy. We used a simple WKB approach to calculate the cross-section for the lowest energy point and the parabolic approximation via the Wong formula [16] for the higher energy points. In this regard we emphasize that the calculated fusion cross-sections do not represent direct TDHF calculations but rather barrier penetration model calculations using the ion-ion potentials obtained above. Also shown are the corresponding experimental values (circles) as well as the barrier penetration model results (dashed line) from Ref. [1]. As anticipated, the calculated cross-sections, with the exception of the lowest energy data point, are now above the corresponding experimental values. There are a number of reasons for overpredicting the data at higher energies. The first reason is the alignment probability of the deformed nucleus, which could be calculated with the availability of the excitation spectrum for the ^{64}Ni nucleus [7]. Physically, one expects a distribution of barriers starting from the lowest barrier and approaching the highest barrier. The second factor is the quality

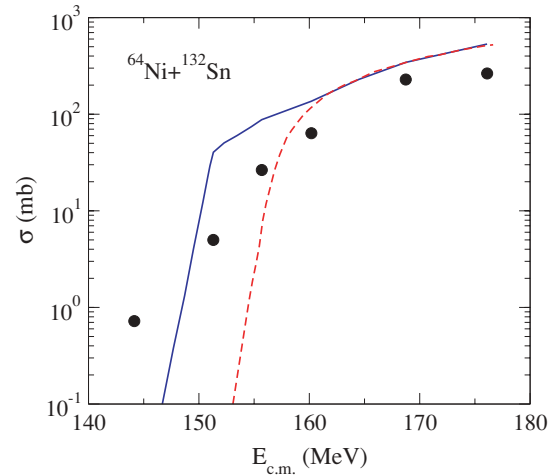


FIG. 2. (Color online) Fusion cross-sections obtained for the $^{64}\text{Ni} + ^{132}\text{Sn}$ system using the microscopically calculated potentials discussed in the manuscript. Also shown (circles) are the experimental values from Ref. [1].

of the parabolic approximation used in the Wong formula. It is well known that the rising Coulomb tail of barriers cannot be properly accounted for by a single parabola, thus resulting in a somewhat thinner barrier and a larger fusion cross-section. In addition, for energies above 160 MeV the fission channel opens up. Finally, despite improving the lowest energy cross-section by many orders of magnitude we find a cross-section of 0.0035 mb, which is still a factor of 200 lower than the experimental value.

In conclusion, we performed microscopic calculations of the interaction potentials for the $^{64}\text{Ni} + ^{132}\text{Sn}$ system. We observe that dynamical deformation effects play a very significant role in the calculation of fusion cross-sections. This observation further underscores the necessity of detailed structure information for neutron and proton rich systems for the better description of fusion cross-sections involving these nuclei. The availability of detailed structure data for the ^{64}Ni nucleus may help explain the discrepancy for the lowest energy point.

This work has been supported by the U.S. Department of Energy under Grant DE-FG02-96ER40963 with Vanderbilt University. Some of the numerical calculations were carried out at the IBM-RS/6000 SP supercomputer of the National Energy Research Scientific Computing Center, which is supported by the Office of Science of the U.S. Department of Energy.

- [1] J. F. Liang *et al.*, Phys. Rev. Lett. **91**, 152701 (2003); **96**, 029903(E) (2006).
 [2] A. B. Balantekin and N. Takigawa, Rev. Mod. Phys. **70**, 77 (1998).
 [3] H. Esbensen, Prog. Theor. Phys. Suppl. **154**, 11 (2004).
 [4] R. G. Stokstad, Y. Eisen, S. Kaplanis, D. Pelte, U. Smilansky, and I. Tserruya, Phys. Rev. Lett. **41**, 465 (1978).

- [5] K. Nishio, H. Ikezoe, S. Mitsuoka, K. Satou, and S. C. Jeong, Phys. Rev. C **63**, 044610 (2001).
 [6] C. Simenel, Ph. Chomaz, and G. de France, Phys. Rev. Lett. **93**, 102701 (2004).
 [7] A. S. Umar and V. E. Oberacker, Phys. Rev. C **74**, 024606 (2006).
 [8] A. S. Umar and V. E. Oberacker, Phys. Rev. C **74**, 021601(R) (2006).

- [9] R. Y. Cusson, P.-G. Reinhard, M. R. Strayer, J. A. Maruhn, and W. Greiner, *Z. Phys. A* **320**, 475 (1985).
- [10] A. S. Umar, M. R. Strayer, R. Y. Cusson, P.-G. Reinhard, and D. A. Bromley, *Phys. Rev. C* **32**, 172 (1985).
- [11] A. S. Umar and V. E. Oberacker, *Phys. Rev. C* **73**, 054607 (2006).
- [12] E. Chabanat, P. Bonche, P. Haensel, J. Meyer, and R. Schaeffer, *Nucl. Phys.* **A635**, 231 (1998); **A643**, 441 (1998).
- [13] J. Dobaczewski, M. V. Stoitsov, and W. Nazarewicz, *Skyrme-HFB Deformed Nuclear Mass Table*, edited by R. Bijker, R. F. Casten, and A. Frank (AIP, New York, 2004), Vol. 726, p. 51.
- [14] G. A. Lalazissis, S. Raman, and P. Ring, *At. Data Nucl. Data Tables* **71**, 1 (1999).
- [15] J. J. Vega, E. F. Aguilera, G. Murillo, J. J. Kolata, A. Morsad, and X. J. Kong, *Phys. Rev. C* **42**, 947 (1990).
- [16] C. Y. Wong, *Phys. Rev. Lett.* **31**, 766 (1973).